Available online at www.sciencedirect.com
SCIENCE DIRECT®
Scripta Materialia 51 (2004) 271–277
Scripta MATERIALIA
www.actamat-journals.com

# Sensitivity of Marangoni convection and weld shape variations to welding parameters in $O_2$–Ar shielded GTA welding

Shanping Lu *, Hidetoshi Fujii, Kiyoshi Nogi

*Joining and Welding Research Institute, Osaka University, 11-1 Mihogaoka, Ibaraki, Osaka 567-0047, Japan*

Received 27 January 2004; received in revised form 25 February 2004; accepted 9 March 2004
Available online 30 April 2004

**Abstract**

The weld metal oxygen content can be significantly changed by a slight difference in the oxygen concentrations in the shielding gas in gas tungsten arc (GTA) welding process. The effects of the welding parameters on the weld shape and depth/width ratio depend to a large extent on the weld metal oxygen content and Marangoni convection patterns.


*Keywords:* Welding; Convection; Oxygen; Mixed shielding gas

## 1. Introduction

In the gas tungsten arc welding process, the weld shape of stainless steel is sensitive to the minor elements, such as sulfur, oxygen and selenium. Adding and precisely controlling the quantity of these minor elements in the weld pool are critical for a satisfactory weld with deep penetration [1–13]. Recent investigations on the effects of oxide flux quantity [14] and active gaseous addition [13] on the weld shape variation showed that the reversal of Marangoni convection pattern was the main mechanism in changing the weld penetration which was first proposed by Bennett, Heiple, Roper and Burgardt [1,2,6,12] in the 1980s.

For the convection controlling GTA liquid pool, heat transfer and fluid flow are driven by a combination of forces including surface tension on the pool surface, electro-magnetic force, buoyancy force and arc plasma drag force. Simulation results by Kou and Wang [15] and Oreper et al. [16] showed that the surface tension and electro-magnetic force dominated the convection mode in the welding pool. In moving GTA weld pool, pattern of Marangoni convection on the pool surface has been widely accepted as the principle mechanism for weld shape variations in the stainless steel with different quantities of minor elements.

Since 1980s, Debroy and co-workers have done many modeling works to study the fluid flow in weld pool for pure iron [17], carbon steel [18,19], and stainless steel [20–23] by laser spot welding or GTA spot welding. Heat transfer and fluid flow not only depend on the thermal properties of the base materials, but also on the power density and welding parameters. Reports by He et al. and Zacharia et al. [20,24], and Wang and Tsai [25] showed that the surface tension for stainless steel with a sulfur content, 240 and 220 ppm, initially increased with temperature and then decreased when the temperature was over 2450 and 2400 K, respectively. When the peak temperature is over these critical temperatures for stainless steel with a high sulfur content, the outward Marangoni convection pattern in the center area will coexist with the inward Marangoni convection pattern at the periphery area on the pool surface. In this case, the active element will not have an appreciable effect on the weld pool shape.

Compared with the research on the effect of sulfur on the weld shape, the role of oxygen in the weld pool on the weld shape is limited. In this study, the effects of the main welding parameters, welding speed, weld current and electrode gap (arc length), on the weld shape in low oxygen added argon shielded GTA welding were investigated on a SUS304 austenitic stainless steel substrate. Based on the weld shape and weld metal oxygen content

* Corresponding author. Tel./fax: +81-06-6879-8663.
*E-mail addresses:* shplu@jwri.osaka-u.ac.jp, shplu@imr.ac.cn (S. Lu).

1359-6462/$ - see front matter 
doi:10.1016/j.scriptamat.2004.03.004

variations with the welding parameters, the effects of oxygen in the weld pool, pattern and magnitude of the Marangoni convection on the weld shape are discussed.

## 2. Experimental

Special SUS304 stainless plates with the average composition of 0.06%C, 0.45%Si, 0.96%Mn, 8.19%Ni, 18.22%Cr, 0.027%P, 0.0005%S, 0.0038%O and the rest of Fe, were selected for the welding experiments and machined into $100\times50\times10$ mm rectangular plates. Two kind of Ar–$O_2$ mixed shielding gases, Ar–0.1vol%$O_2$ and Ar–0.3vol%$O_2$, were selected in the welding experiments under flow rate 10 l/min. The mixed shielding gas was prepared from pure argon and a premixed 1.0vol%$O_2$–Ar gases. All partial penetrate, 50 mm length bead-on-plate welds were made with a direct current, electrode negative (DCEN) GTAW power supply.

A water-cooled torch with $\phi$ 2.4 mm, W–2%$ThO_2$ electrode was used. It was fixed above the horizontally positioned weld plate, which can move at different speed with a mechanized system. The details of the thermal properties of stainless steel and the welding parameters are listed in Table 1.

After welding, specimens for the weld shape observation were prepared and etched by an $HCl + Cu_2SO_4$ solution to reveal the bead shape and size. The cross-sections of the weld bead were photographed using an optical microscope. The oxygen content in the weld metal was analyzed using an oxygen/nitrogen analyzer (Horiba, EMGA-520).

## 3. Results and discussion

### 3.1. Convection and conduction in liquid pool

Generally, the heat transfer in the liquid pool occurs in the combination of convection and conduction modes. Relative importance between heat convection and conduction, which can be valued by Peclet number, varies for different materials [26–28]. Peclet number representing the ratio of heat transfer by convection and conduction was defined as follows:

$$Pe = \frac{L \cdot V_{\max}}{2\alpha_l} \tag{1}$$

where, $V_{\max}$ is the maximum surface velocity, $\alpha_l$ is the thermal diffusivity of liquid and $L$ is the characteristic length of the weld pool, which can be taken as the weld pool surface radius for wide and shallow weld pool without or with low active element content. In the deep and narrow weld pool containing certain active element, $L$ can be taken as the depth of the weld pool [18].

For the results under welding current, 160 A, welding speed, 2.0 mm/s and electrode gap, 3 mm, the weld pool is shallow and wide with the pool surface width, 8.84 mm for Ar–0.1vol%$O_2$ shielding gas. Under Ar–0.3vol%$O_2$ shielding, the weld metal oxygen content is 127 ppm and the weld shape is narrow and deep with the pool depth, 3.75 mm. Zacharia et al. [20] theoretically calculated the maximum velocity for SUS304 stainless steel is 0.12 m/s by stationary GTA welding. Using the thermal data in Table 1 and supposing that the maximum velocity on pool surface is 0.12 m/s, the Peclet numbers by Eq. (1) are 68 and 58 for Ar–0.1vol%$O_2$ and Ar–0.3vol%$O_2$, respectively. The high Peclet number signifies that heat transfer in liquid pool in this study is dominated by convection mode.

Table 1
Thermal properties [25] of SUS304 and welding parameters

| Nomenclature | Values |
|---|---|
| Density, $\rho$ (kg/m$^3$) | 7200 |
| Dynamic viscosity, $\mu$, (kg m$^{-1}$ s$^{-1}$) | 0.006 |
| Specific heat of liquid, $C_{pl}$, (J kg$^{-1}$ K$^{-1}$) | 780 |
| Thermal conductivity of liquid, $K_l$, (J m$^{-1}$ s$^{-1}$ K$^{-1}$) | 22 |
| Thermal diffusivity of liquid, $\alpha_l = K_l/\rho C_{pl}$, (m$^2$ s$^{-1}$) | $3.9\times10^{-6}$ |
| Electrode gap (mm) | 1–9 |
| Welding current (A) | 60–260 |
| Welding speed (mm/s) | 0.75–5 |

### 3.2. Effect of welding speed on weld shape

The weld depth/width ($D/W$) ratio, weld metal oxygen content and weld shapes are shown in Figs. 1 and 2, respectively, under different welding speed from 0.75 to 5.0 mm/s. The weld $D/W$ ratio decreases with the increasing welding speed for the Ar–0.3vol%$O_2$ shielding gas. For the Ar–0.1vol%$O_2$ shielding gas, the weld $D/W$ ratio remains constant at around 0.2. Weld metal oxygen contents are over 120 ppm and around 30 ppm for the Ar–0.3vol%$O_2$ and Ar–0.1vol%$O_2$ shielding gases, respectively. When the oxygen content in the weld

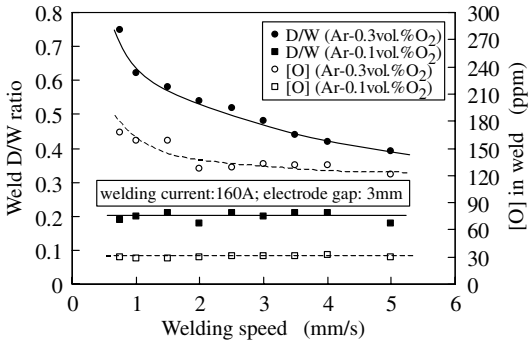


Fig. 1. Effect of welding speed on weld $D/W$ ratio and weld metal oxygen content for Ar–0.3vol%$O_2$ and Ar–0.1vol%$O_2$ shielding gases.

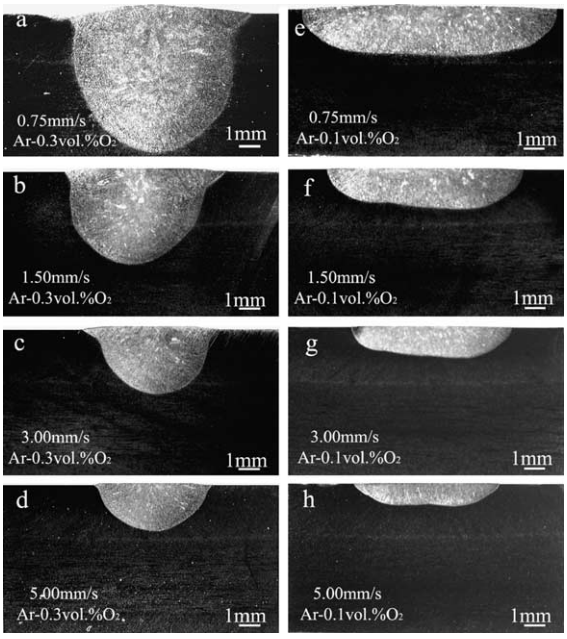


Fig. 2. Weld shapes at different welding speeds for Ar–0.3vol%$O_2$ and Ar–0.1vol%$O_2$ shielding gases.

metal is over the critical value of around 100 ppm, the Marangoni convection pattern will change from an outward direction to an inward direction in moving GTA welding [13,14]. Therefore, an inward Marangoni convection for the Ar–0.3vol%$O_2$ shielding gas and outward Marangoni convection for the Ar–0.1vol%$O_2$ shielding gas occur in welding process. When the heat transfer in weld pool occurs mainly by convection, the weld shape depends to a large extent on the direction and magnitude of Marangoni convection controlled by the surface tension on the weld pool surface.

By dimensionless analysis, the intensity of surface tension driven convection can be measured by Marangoni number, *Ma*, which is defined as [27,28]:

$$Ma = \frac{\frac{d\sigma}{dT} \cdot L \cdot \Delta T}{2\mu\alpha_l} = \frac{\frac{d\sigma}{dT}\frac{dT}{dr} \cdot r \cdot L}{2\mu\alpha_l} \tag{2}$$

where $d\sigma/dT$ is the temperature coefficient of the surface tension, $r$ is the radius of the pool surface, $dT/dr$ is the temperature gradient on the pool surface, $\mu$ is the dynamic viscosity, and $\rho$ is the density. Based on the modeling results on heat transfer and fluid flow in weld pool for gallium, pure aluminum, aluminum alloy, pure iron, steel titanium and sodium nitrate, Robert and Debroy [28] proposed a general applicable relationship between Peclet and Marangoni number as following

$$Pe = 0.08Ma^{0.93} \tag{3}$$

For the surface tension is the dominant driving force for convection on pool surface, the maximum velocity, $V_{max}$, on pool surface can be approximated by [29]

$$V_{max}^{3/2} = \frac{d\sigma}{dT} \cdot \frac{dT}{dr} \cdot \frac{L^{1/2}}{0.664\rho^{1/2}\mu^{1/2}} \tag{4}$$

Substituting Eq. (4) into Eq. (1), the *Pe* number can be given as

$$Pe = \frac{\left(\frac{d\sigma}{dT}\frac{dT}{dr}\right)^{2/3} \cdot L^{4/3}}{1.52\alpha_l \cdot \rho^{1/3} \cdot \mu^{1/3}} \tag{5}$$

$(d\sigma/dT)(dT/dr)$ can be defined as the surface tension stress $\tau_{s.t}$. Assuming that the relation between Peclet number and Marangoni number in Eq. (3) can be applied for stainless steel here and substituting the Eqs. (2) and (5) into Eq. (3), the surface tension stress, $\tau_{s.t}$, can be estimated by

$$\tau_{s.t} = \frac{d\sigma}{dT}\frac{dT}{dr} = 3.5 \times 10^4 \times \frac{\mu^{2.27}}{\alpha_l^{0.27} \cdot \rho^{1.27}} \cdot \frac{L^{1.53}}{r^{3.53}} \tag{6}$$

Using the thermal properties listed in Table 1 and the weld pool size in Fig. 2, the surface tension stress, $\tau_{s.t}$, is calculated and plotted versus the welding speed in Fig. 3.

The sign of surface tension stress indicates the direction of Marangoni convection on pool surface. Positive value means inward convection and negative value means outward convection. The magnitude of the surface tension stress determines the strength of the Marangoni convection on the liquid pool. It is clear in Fig. 3 that the surface tension stress decreases with the increasing welding speed under Ar–0.3vol%$O_2$ shielding because higher welding speed will decrease the heat input per unit length of the weld bead, the peak temperature on pool surface and the temperature gradient. Lower surface tension stress will weaken the inward Marangoni convection on pool surface and decreases the weld $D/W$ ratio with the increasing welding speed as shown in Fig. 1. However, for the outward Marangoni convection pattern under Ar–0.1vol%$O_2$ shielding gas, it is interesting to find that the magnitude of the surface tension stress increases with the increasing of the welding speed as shown in Fig. 3. Low temperature gradient under high welding speed will weaken the outward

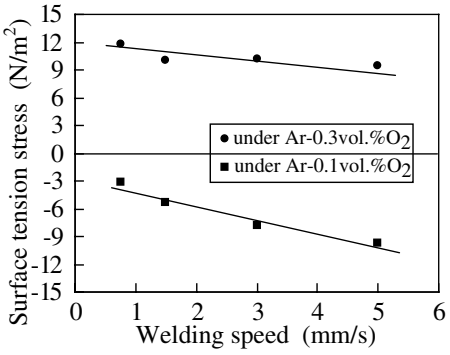


Fig. 3. Effect of welding speed on Surface tension stress.

Marangoni convection and lead to a decreasing the weld width, which will impede the decrease in the surface temperature gradient. Therefore, the surface tension stress does not decrease with the increasing of the welding speed under Ar–0.1vol%$O_2$ shielding. The magnitude of the surface tension stress under Ar–0.1vol%$O_2$ is lower than that under Ar–0.3vol%$O_2$. So the outward Marangoni convection under Ar–0.1vol%$O_2$ is weaker than inward Marangoni convection under Ar–0.3vol%$O_2$. Furthermore, the high welding speed will decrease the heat input per unit length of the weld bead, so the weld $D/W$ ratio under Ar–0.1vol%$O_2$ is not sensitive to the welding speed and remains around 0.2 as shown in Fig. 1. The results are in good agreement with the findings by Burgardt and Heiple [30], Shirali and Mills [31] about the effect of the welding speed on the weld shape for stainless steel with different sulfur contents.

The weld cross section areas were measured as shown in Table 2 under different oxygen addition shielding gas with welding current, 160 A, and welding speed, 2.0 mm/s, [13]. Cross section areas are relatively larger under Ar–(0.3–0.5)vol%$O_2$ shielding, which means that the heat transfer efficiency is relatively higher. The heat transfer efficiency directly controls the weld pool volume. However, the weld pool shape is mainly controlled by the convection pattern and magnitude. Even at the same heat transfer efficiency under Ar–(0–0.2)vol%$O_2$ and Ar–(0.7–1.0)vol%$O_2$ shielding, the weld shapes are different [13].

### 3.3. Effect of welding current on weld shape

Compared with the welding speed, the welding current is a complex parameter. Changing the welding current will directly alter the heat input and weld area. The heat distribution of the arc on the weld pool is a main factor affecting the weld shape and weld $D/W$ ratio. Tsai and Eagar [32] observed that increasing the welding current would increase the magnitude of the heat intensity and widen the heat distribution of the arc on the pool surface. However, the heat distribution width weakly increases compared with the magnitude of the heat density. The higher the magnitude of the heat density, the larger is the temperature gradient on the pool surface. The temperature coefficient of surface tension on pool surface depends not only on the surface active element content in weld pool, but also on the temperature distribution. Large welding current leads to high peak temperature on pool surface. It is possible

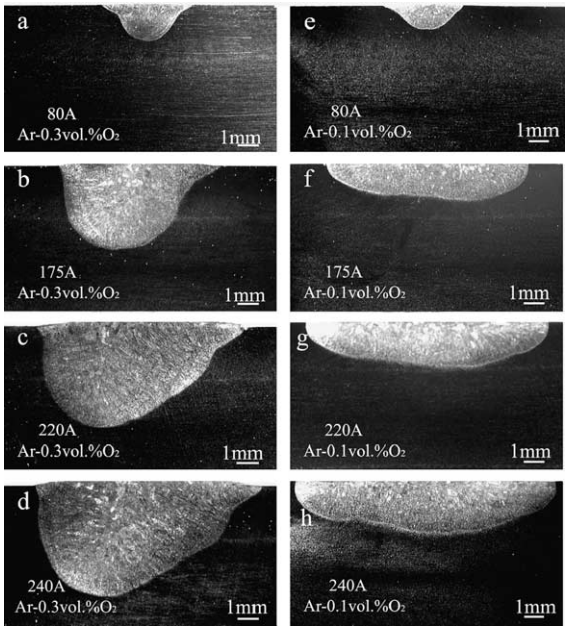


Fig. 4. Weld shapes at different welding currents for Ar–0.3vol%$O_2$ and Ar–0.1vol%$O_2$ shielding gases.

that a complex bifurcated flow pattern with radial outward on pool center and inward loop at periphery area coexists on pool surface when the peak surface temperature is beyond a particular temperature [20,21,24]. On the other hand, the large welding current will also increase the electro-magnetic force, which strengthens the downward body convection in the welding pool and increase the weld $D/W$ ratio.

Fig. 4 shows the effect of welding current on the weld shapes. All the weld shapes are relatively deep and narrow under Ar–0.3vol%$O_2$ shielding as shown in Fig. 4(a,b,c,d).

Wide and shallow weld shapes form at high welding currents under Ar–0.1vol%$O_2$ shielding as shown in Fig. 4(f,g,h). However, Fig. 4(e) shows that the weld shape is relative narrow and deep under low welding current. It is supposed here that the dominant Marnagoni convection is inward direction for the deep and narrow weld shapes, and outward direction for the wide and shallow weld pools.

Figs. 5 and 6 show the weld depth/width and weld metal oxygen content under different welding currents, respectively. The weld $D/W$ ratio initially increases, followed by a slightly decreasing with the increasing welding current under Ar–0.3vol%$O_2$ shielding as shown in Fig. 5. Under Ar–0.1vol%$O_2$ shielding, the weld $D/W$ decreases weakly with the increasing current.

Table 2
Weld pool area under different torch gas oxygen content [13]

| Oxygen content (vol%) | 0 (Pure Ar) | 0.1 | 0.2 | 0.3 | 0.4 | 0.5 | 0.7 | 0.9 |
|---|---|---|---|---|---|---|---|---|
| Weld pool area ($mm^2$) | 10.1 | 10.8 | 12.9 | 16.7 | 16.6 | 15.2 | 9.1 | 9.1 |

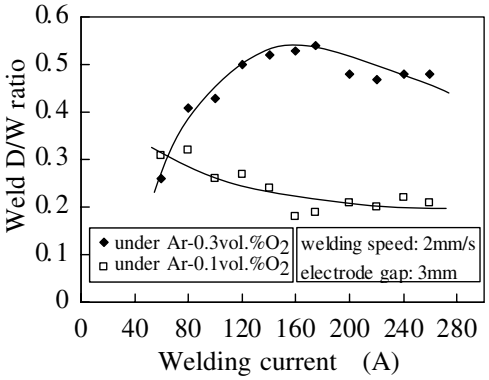


Fig. 5. Effect of welding current on weld $D/W$ ratio.

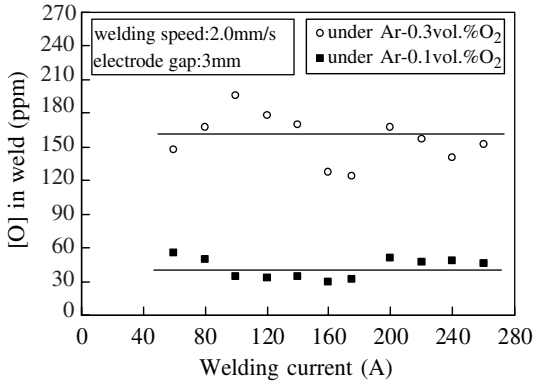


Fig. 6. Effect of welding current on weld metal oxygen content.

Table 3
Surface tension stress, $\tau_{s.t}$, for different welding currents

| Current (A) | 80 | 175 | 220 | 240 |
|---|---|---|---|---|
| $\tau_{s.t}$ (N/m$^2$) (0.3vol%$O_2$) | +17.3 | +8.4 | +3.9 | +3.5 |
| $\tau_{s.t}$ (N/m$^2$) (0.1vol%$O_2$) | +17.0 | −5.0 | −3.4 | −2.9 |

Using Eq. (6), the surface tension stresses were calculated and given in Table 3. Surface tension stress decreases with the increasing welding currents under Ar–0.3vol%$O_2$ shielding. Fig. 6 shows that the weld metal oxygen content is around 160 ppm under Ar–0.3vol%$O_2$ shielding. Since the Fe, Ni and Cr have very similar surface tension and atomic dimensions and form nearly ideal solutions [33], the effect of oxygen on surface tension of stainless steel can be taken using the data of Fe–O system as a reference. When the oxygen content is around 160 ppm, the critical temperature for positive temperature coefficient of surface tension to negative one is around 2200 K [34]. Under high welding current, the weld pool peak temperature is possibly over 2200 K, and outward Marangoni convection on pool center coexists with the inward convection at periphery area of the pool surface. Due to the outward convection in limited pool center area under high welding current, the overall inward convection was weakened and the equivalent surface tension stress for the inward convection decreases at high welding current as shown in Table 3 under Ar–0.3vol%$O_2$ shielding. Therefore, the weld $D/W$ ratio decreases slightly at high welding current as shown in Fig. 5. However, for moving GTA welding, the peak temperature will not be so high as that under the laser spot welding and the inward convection at periphery area is still the dominant one on pool surface, which makes the weld shapes relatively deep and narrow under Ar–0.3vol%$O_2$ shielding. On the other hand, the larger the welding current, the stronger the weld pool body convection by electro-magnetic force. So the weld $D/W$ ratio initially increases with the welding current under Ar–0.3vol%$O_2$ shielding. Under Ar–0.1vol%$O_2$ shielding, the weld metal oxygen content is around 40 ppm as shown in Fig. 6. Based on the temperature coefficient of surface tension of Fe–O system [34], when the oxygen content is lower than 20 ppm, the temperature coefficient of surface tension is always negative. When the oxygen content is around 40 ppm, temperature coefficient of surface tension is positive at relative low temperature (<1950 K). Theoretically, there should be a small inward convection at pool edge. When the welding current is very low, the peak temperature on pool surface is low and the pool edge inward convection plays an important role on the weld pool shape, which make the weld pool is relatively narrow and deep as shown in Fig. 4(e) and the weld $D/W$ is relatively high compared to that at large welding current under Ar–0.1vol%$O_2$. When the welding current is increasing, the peak temperature increases and the pool center outward convection overwhelms the small inward convection at pool edge. Ultimately, the weld shapes become wide and shallow as shown in Fig. 4(e,f,g).

### 3.4. Effect of electrode gap on the weld shape

The role of the electrode gap in determining the weld shape was studied by varying the arc length from 1.0 to

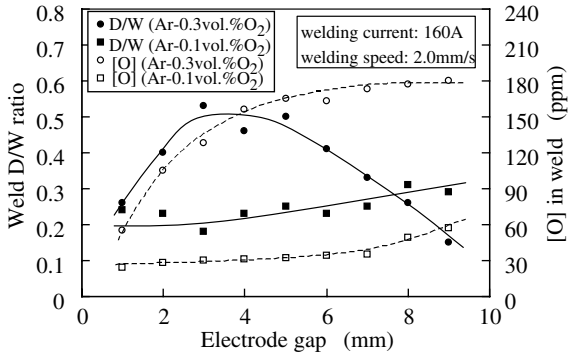


Fig. 7. Effect of electrode gap on weld $D/W$ ratio and weld metal oxygen content for Ar–0.3vol%$O_2$ and Ar–0.1vol%$O_2$ shielding gases.

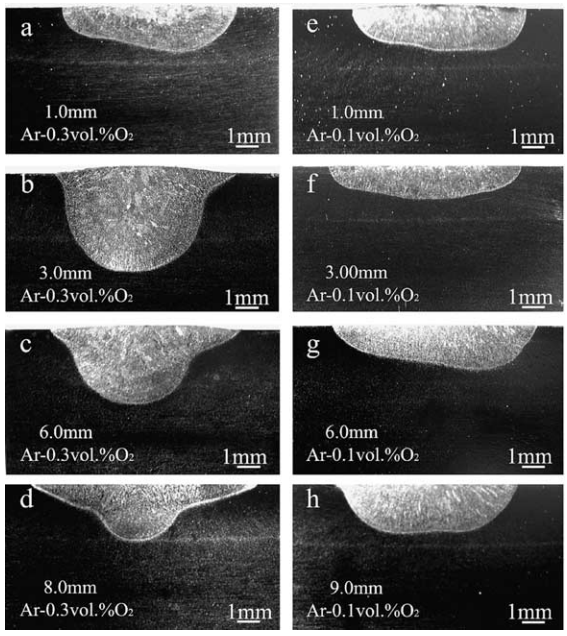


Fig. 8. Weld shapes for different electrode gaps for Ar–0.3vol%$O_2$ and Ar–0.1vol%$O_2$ shielding gases.

9.0 mm as shown in Figs. 7 and 8. Under the Ar–0.3vol%$O_2$ shielding gas, the weld $D/W$ ratio initially increases and then decreases with the increasing electrode gap. However, under the Ar–0.1vol%$O_2$ shielding gas, the weld $D/W$ slightly increases with the electrode gap. At a constant welding current, the large electrode gap will directly increase the arc length and the arc voltage. Therefore, the overall heat supply from the welding power system will increase when the electrode gap becomes large. However, the arc efficiency will reduce when the arc length increases [30]. Tsai reported that a large electrode gap will broaden the heat distribution of the arc on the weld pool surface significantly [32], which will enlarge the anode size and lower the heat density on the pool. Therefore, the temperature gradient on the pool surface decreases when the electrode gap increases. Ultimately, the Marangoni convection on the pool surface weakens. Based on these facts, the weld $D/W$ ratio should decrease for the inward Marangoni convection pattern and increase for the outward Marangoni convection pattern with an increase in the electrode gap.

However, under the Ar–0.3vol%$O_2$ shielding gas, the weld $D/W$ ratio first increased, followed by a decrease with an increase in the electrode gap. It is interesting to find that the weld metal oxygen content increases with the electrode gap both for the Ar–0.3vol%$O_2$ and Ar–0.1vol%$O_2$ shielding gases. The oxygen content in the weld metal is mainly from the decomposition of $O_2$ in the arc column and its adsorption to the liquid pool. The larger the electrode gap, the larger the arc column area and heat supply, which strengthens the decomposition of $O_2$ in the arc plasma, and hence increases the oxygen content adsorption in the liquid pool. Also, the increase in the weld width will increase the reaction area between oxygen and the weld pool, and hence increase the oxygen content in weld metal. When the electrode gap is set at 1 mm, the weld metal oxygen content is about 55 ppm for the Ar–0.3vol%$O_2$ shielding gas, which is relatively lower value under Ar–0.3vol%$O_2$ shielding. For this case, the weld pool inward convection at edge is weak and the outward convection on pool center is dominant, so the weld shape is wide and shallow as shown in Fig. 8(a) and the weld $D/W$ is small, which is quite different from the weld shapes as shown in Fig. 8(b,c,d) where inward convection is dominant. Because of the different Marangoni convection mode, the weld $D/W$ ratio increases initially under the Ar–0.3vol%$O_2$ shielding gas as shown in Fig. 7.

Table 4
Surface tension stress, $\tau_{s.t} = (d\sigma/dT)(dT/dr)$, for different electrode gaps

| Gap (mm) | 1 | 3 | 6 | 8 | 9 |
|---|---|---|---|---|---|
| $\tau_{s.t}$ (N/m$^2$) (0.3vol.%$O_2$) | −8.0 | +10.5 | +5.3 | +1.6 | |
| $\tau_{s.t}$ (N/m$^2$) (0.1vol.%$O_2$) | −8.1 | −6.0 | −5.8 | | −7.1 |

The surface tension stress is calculated by Eq. (6) and given in Table 4. Under Ar–0.3vol%$O_2$ shielding, the surface tension stress decreases with the increasing of the electrode gap from 3 mm. So the inward Marangoni convection weakens and the weld $D/W$ ratio decreases with the increasing electrode gap over 3 mm under Ar–0.3vol%$O_2$ shielding as shown in Fig. 7. As mentioned above, the temperature gradient will decrease with the increasing electrode gap, so the outward Marangoni convection will weaken under Ar–0.1vol%$O_2$ shielding. However, the weakened outward convection will decrease the weld width, which will impede the decrease of the temperature gradient on pool surface. Therefore, the surface tension stress is not sensitive to the electrode gap under Ar–0.1vol%$O_2$ shielding as shown in Table 4.

## 4. Conclusions

A minor element, oxygen, in the weld pool can be adjusted by the mixing of oxygen gas in the argon base shielding gas in GTA welding. In moving GTA welding on SUS304 stainless steel, the heat transfer and fluid flow in weld pool occurs mainly by convection mode. Marangoni convection patterns on the pool surface are controlled by the combination of the oxygen content and the temperature distribution on pool surface, which depends to large extent on the welding parameters.

Surface tension stress, $\tau_{s.t} = (d\sigma/dT)(dT/dr)$, can be estimated by the weld pool size and explains the Marangoni convection phenomena on weld pool surface. A slightly difference in the weld metal oxygen content from

different shielding gases introduces a significantly different response in the weld $D/W$ ratio to the variant welding parameters. The weld $D/W$ ratio under the Ar–0.3vol%$O_2$ shielding gas substantially depends on the welding variables. However, the weld $D/W$ ratio under the Ar–0.1vol%$O_2$ shielding gas is not sensitive to the different welding parameters.

## Acknowledgements

This work is the result of "Development of Highly Efficient and Reliable Welding Technology", which is supported by the New Energy and Industrial Technology Development Organization (NEDO) through the Japan Space Utilization Promotion Center (JSUP) in the program of Ministry of Economy, Trade and Industry (METI), the 21st Century COE Program, ISIJ research promotion grant, and JFE 21st Century Foundation.

## References

[1] Bennett WS, Mills GS. Weld J 1974;53:548s.
[2] Heiple CR, Roper JR. Weld J 1981;60:143s.
[3] Takeuch Y, Takagi R, Shinoda T. Weld J 1992;71:283s.
[4] Tanaka M, Shimizu T, Terasaki H, Ushio M, Koshi-ishi F, Yang CL. Sci Technol Weld Joi 2000;5:397.
[5] Howse DS, Lucas W. Sci Technol Weld Joi 2000;5:189.
[6] Heiple CR, Roper JR. Weld J 1982;61:97s.
[7] Lucas W, Howse D. Weld Met Fabr 1996;64:11.
[8] Paskell T, Lundin C, Castner. Weld J 1997;76:57s.
[9] Wang Y, Tsai HL. Metall Mater Trans B 2001;32:501.
[10] Bad'yanov BN, Davdov VA, Ivanov VA. Avtom Svarka 1974; 11:1.
[11] Bad'yanov BN. Avtom Svarka 1975;1:74.
[12] Heiple CR, Burgardt P. Weld J 1985;64:159s.
[13] Lu SP, Fujii H, Sugiyama H, Tanaka M, Nogi K. ISIJ Int 2003; 43:1590.
[14] Lu SP, Fujii H, Sugiyama H, Tanaka M, Nogi K. Mater Trans 2002;43:2926.
[15] Kou S, Wang YH. Weld J 1986;65:63s.
[16] Oreper GM, Eagar TW, Szekely J. Weld J 1983;62:307s.
[17] Paul A, Debroy T. Metall Trans 1988;19B:851.
[18] Pitscheneder W, Debroy T, Mundra K, Ebner R. Weld J 1996;75:71s.
[19] Zhang W, Roy GG, Elmer JW, Debroy T. J Appl Phys 2003;93: 3022.
[20] Zacharia T, David SA, Vitek JM, Debroy T. Weld J 1989;68:499s.
[21] Zacharia T, David SA, Vitek JM, Debroy T. Weld J 1989;68:510s.
[22] He X, Fuerschbach PW, Debroy T. J Phys D: Appl Phys 2003; 36:1388.
[23] Mundra K, Debroy T. Metall Trans 1993;24B:145.
[24] Zacharia T, David SA, Vitek JM, Debroy T. Metall Trans 1990; 21B:600.
[25] Wang Y, Tsai HL. Int J Heat Mass Trans 2001;44:2067.
[26] Oreper GM, Szekely J. Metall Trans 1987;18A:1325.
[27] Limmaneevichitr C, Kou S. Weld J 2000;79:231s.
[28] Robert A, Debroy T. Metall Mater Trans 2001;32B:941.
[29] Debroy T, David SA. Rev Mod Phys 1995;67:85.
[30] Burgardt P, Heiple R. Weld J 1986;65:150s.
[31] Shirali AA, Mills KC. Weld J 1993;72:347s.
[32] Tsai NS, Eagar TW. Metall Trans B 1985;16:841.
[33] Mcnallan MJ, Debroy T. Metall Trans 1991;22B:557.
[34] Sahoo P, Debroy T, Mcnallan MJ. Metall Trans 1988;19B:483.